POLITECNICO DI TORINO
Repository ISTITUZIONALE

A Multivariate Adaptive Sampling Scheme for Passivity Characterization of Parameterized Macromodels

(Article begins on next page)

18 October 2022

A Multivariate Adaptive Sampling Scheme for Passivity Characterization of Parameterized Macromodels

Marco De Stefano, Stefano Grivet-Talocia

Dept. Electronics and Telecommunications, Politecnico di Torino, Italy

Abstract—We introduce a multivariate adaptive sampling algorithm for the passivity characterization of parameterized macromodels. The proposed approach builds on existing sampling methods based on adaptive frequency warping for tracking pole-induced variability of passivity metrics, which however are available only for univariate (non-parameterized) models. Here, we extend this approach to the more challenging parameterized setting, where model poles hence passivity violations depend on possibly several external parameters embedded in the macromodel. Numerical examples show excellent performance and speedup with respect to competing approaches.

I. Introduction

Behavioral models of complex interconnects are now a commodity in modern Signal and Power Integrity design verification flows. Numerical simulation of complex large-scale interconnects with their terminations greatly benefits from reduced-complexity macromodels of devices of subsystems, whose extraction is performed through dedicated tools from CAD vendors. These tools are now mature and robust [1].

A different scenario applies to early stages of the design, where different solutions, layouts, component choices are tested in order to choose the optimal configuration. In this situation, different and independent macromodels must be extracted anytime the system under modeling is modified. It is thus beneficial to construct scalable multivariate macromodels that embed not only frequency dependence, but also one or more design parameters in a compact closed form. Once extracted from field solver data, such models can be instantiated for any arbitrary value of these parameters directly through a parameterized SPICE netlist, allowing significant savings in computing and human time resources.

Multivariate macromodeling has been revitalized in recent years, and several major improvements have been documented. These include an appropriate model structure for representing parameter-induced variability in the model poles [2], [3], efficient uniform stability constraints [4], multivariate passivity verification and enforcement [5], and good scalability to large port counts [6]. One aspect that still deserves attention is the passivity verification, which is essential for setting up a passivity enforcement loop that corrects model violations to ensure time stability in system-level transient simulations. Although advanced solutions exist for multivariate passivity verification, they are characterized by large computational complexity and poor scalability with model size and especially number of independent parameters. This is essentially due to the need of resorting to repeated eigensolutions of suitably-defined Hamiltonian matrices/pencils.

In this work, we propose a novel multivariate adaptive sampling scheme, which generalizes the method of [6] to the multivariate case. The main idea is to completely avoid Hamiltonian matrices in order to reduce runtime. Passivity violations are detected by a two-step adaptive sampling that: i) tracks fast variations through a pole-based initial subdivision of the frequency axis into nonuniformly-distributed subbands, where local variations are predictably smooth; ii) processes each independent subband through a mesh refinement based on hierarchical tree subdivision. The results of [6] show that with a proper implementation, this scheme is at least as accurate as Hamiltonian-based verification methods, providing much improved scalability for large-scale models. Here, we extend this approach to the parameterized setting, where fast variations need to be tracked not only along frequency, but throughout a possibily high-dimensional parameter space.

II. Two-Step Multivariate Adaptive Sampling

Let us consider a parameterized macromodel with transfer function $\mathbf{H}(s, \boldsymbol{\vartheta}) \in \mathbb{C}^{P \times P}$, where s is the Laplace variable and $\boldsymbol{\vartheta} = [\vartheta^1, \vartheta^2, ..., \vartheta^\rho]^\mathsf{T}$ collects a set of ρ independent parameters such as geometrical dimensions, material characteristics, temperature, etc. defined within a parameter space

$$\Theta = [\vartheta_{\min}^1, \vartheta_{\max}^1] \times [\vartheta_{\min}^2, \vartheta_{\max}^2] \times \cdots \times [\vartheta_{\min}^\rho, \vartheta_{\max}^\rho]. \quad (1)$$

It is assumed that this model is available from one of the many available multivariate model extraction methods, such as [2], [3], [4]. The proposed approach does not assume a particular model structure and is thus of general applicability as a post-processing tool for passivity verification. The only two requirements are: i) evaluation of $\mathbf{H}(s, \boldsymbol{\vartheta})$ for any given $(s, \boldsymbol{\vartheta})$ is fast, and ii) once $\boldsymbol{\vartheta}$ is fixed, the (parameter-dependent) poles $p_n(\boldsymbol{\vartheta})$ of the model in a standard pole-residue expansion

$$\mathbf{H}(s, \boldsymbol{\vartheta}) = \sum_{n=1}^{\bar{n}} \frac{\mathbf{R}_n(\boldsymbol{\vartheta})}{s - p_n(\boldsymbol{\vartheta})} + \mathbf{R}_0(\boldsymbol{\vartheta}) \quad (2)$$

are easily extracted. Note that (2) with the explicit parameterization of the poles is not appropriate, and usual model structures embed pole variability in implicit form through a parameterized Sanathanan-Koerner or state-space/descriptor

form [5]. Assuming a model with uniformly stable poles $\text{Re}\{p_n(\boldsymbol{\vartheta})\} < 0$, $\forall\boldsymbol{\vartheta}$, passivity holds if the *passivity metric*

$$\phi(\omega, \boldsymbol{\vartheta}) \geq 0 \quad \forall\omega \in \mathbb{R} \quad \forall\boldsymbol{\vartheta} \in \Theta \tag{3}$$

where, depending on the model representation,

$$\phi(\omega, \boldsymbol{\vartheta}) = \begin{cases} 1 - \sigma_{\max}\{\mathbf{H}(\mathrm{j}\omega; \boldsymbol{\vartheta})\} & \text{scattering} \\ \lambda_{\min}\{\mathbf{H}(\mathrm{j}\omega; \boldsymbol{\vartheta}) + \mathbf{H}(\mathrm{j}\omega; \boldsymbol{\vartheta})^{\mathsf{H}}\} & \text{immittance} \end{cases} \tag{4}$$

where $\sigma_{\max}$ and $\lambda_{\min}$ are the largest singular value and the smallest eigenvalue, respectively. The proposed approach aims at detecting all negative local minima of $\phi(\omega, \boldsymbol{\vartheta})$, i.e. the worst-case local passivity violations.

A. Tracking pole-induced variability along frequency

Let us start by freezing the parameters as $\boldsymbol{\vartheta} = \boldsymbol{\vartheta}_\alpha$, and let us denote the poles of the univariate model $\mathbf{H}(s, \boldsymbol{\vartheta}_\alpha)$ as $p_n^\alpha = \sigma_n^\alpha \pm \mathrm{j}\omega_n^\alpha$. Following [6], we define the *control points*

$$\{\hat{\omega}_\nu^\alpha\} = \mathcal{C}\left(\bigcup_{n=1}^{\bar{n}} \bigcup_{r=-R}^{R} \left\{\omega_n^\alpha + \sigma_n^\alpha \tan\frac{r\pi}{2(R+1)}\right\}\right), \tag{5}$$

where operator $\mathcal{C}$ removes negative samples and sorts in ascending order, and where R is a small integer. We split the frequency axis into disjoint subbands

$$\Omega = [0, +\infty) = \bigcup_{\nu=0}^{\bar{\nu}(\alpha)-1} \Omega_\nu^\alpha, \quad \Omega_\nu^\alpha = [\hat{\omega}_\nu^\alpha, \hat{\omega}_{\nu+1}^\alpha) \tag{6}$$

where $\hat{\omega}_0^\alpha = 0$ and $\hat{\omega}_{\bar{\nu}(\alpha)}^\alpha = +\infty$. We refer to [6] for the minor modifications that are required to handle real poles.

A nonlinear frequency warping is then performed by applying a piecewise linear and invertible change of variable $\zeta^\alpha = \mathcal{W}_\alpha(\omega)$ mapping each subband as

$$\Omega_\nu^\alpha \xrightarrow{\mathcal{W}_\alpha} \Xi_\nu^\alpha = [\nu, \nu+1) \tag{7}$$

As discussed in [6], this change of variables plays the role of "flattening" sharp variations in the new domain ζ^α. Since the control points track the peaks of the resonance curves associated to the poles, which are the main responsible for fast variations in the singular value or eigenvalue trajectories, it is argued that the passivity metric

$$\eta_\alpha(\zeta^\alpha) = \eta(\zeta^\alpha, \boldsymbol{\vartheta}_\alpha) = \phi(\mathcal{W}_\alpha^{-1}(\zeta^\alpha), \boldsymbol{\vartheta}_\alpha) \tag{8}$$

has local variations that are almost uniform in each normalized subband Ξ_ν^α. The advantages of this transformation are graphically illustrated in Fig. 1.

B. Tracking pole-induced variability in the parameter space

The above frequency transformation depends on the choice of a specific parameter value $\boldsymbol{\vartheta}_\alpha$ and is valid only at this particular point. The next step towards tracking the variability of the passivity metric throughout parameter space is to choose a set of values $\{\boldsymbol{\vartheta}_\alpha, \alpha = 1, \ldots, \bar{\alpha}\}$ that cover the entire parameter space, and that will be used to discretize the
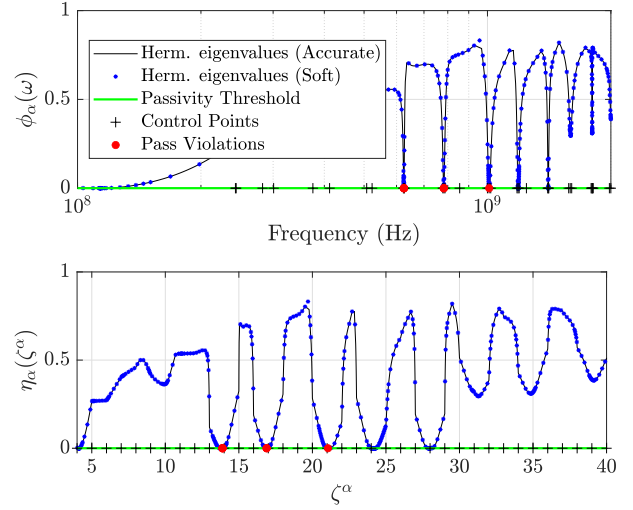

Fig. 1. Passivity metric in the natural frequency domain (top; solid line: fine sweep, dots: proposed scheme in a *fast/soft* mode [6]) and after frequency warping (bottom), resulting in a better resolution in detection of local minima.

continuous parametric dependence of the model poles. In this preliminary work, we introduce a tessellation

$$\Theta = \bigcup_{\alpha=1}^{\bar{\alpha}} \Theta_\alpha \tag{9}$$

where Θ_α are disjoint hyper-rectangles from a uniform subdivision of each direction θ^ℓ into μ_ℓ intervals for $\ell = 1, \ldots, \rho$. This choice leads to a total number $\bar{\alpha} = \prod_{\ell=1}^{\rho} \mu_\ell$. Other choices are possible, e.g. through high-dimensional simplexes. We denote with $\boldsymbol{\vartheta}_\alpha$ the centroid of each subdomain Θ_α.

Figure 2 provides a graphical representation of this tessellation for the one-dimensional case $\rho = 1$, where both Θ and Θ_α are intervals. The vertical solid black lines represent the control points, which provide a piecewise constant discretization throughout Θ_α of the resonance frequencies of the poles and their induced samples as defined in (5) (thick red lines), evaluated at $\boldsymbol{\vartheta}_\alpha$. Each rectangle in the figure represents a $(\rho+1)$-dimensional hyperrectangle

$$\Psi_{\alpha,\nu} = \Theta_\alpha \times \Omega_\nu^\alpha \tag{10}$$

The size of these subdomains and their distribution along the frequency axis tracks the fast variations of the passivity metric under investigation.

C. Hierarchical subdomain sampling

The next step is an independent processing of all individual subdomains $\Psi_{\alpha,\nu}$. The total number of these subdomains is $\sum_{\alpha=1}^{\bar{\alpha}} \bar{\nu}(\alpha)$, which can be large. Since all these subdomains will be processed independently, the proposed scheme is straightforward to implement on a parallel computing architecture, this is left for future investigations. Each subdomain is mapped to the unit hypercube through a basic rescaling/shifting operator $\mathcal{S}_{\alpha,\nu}$

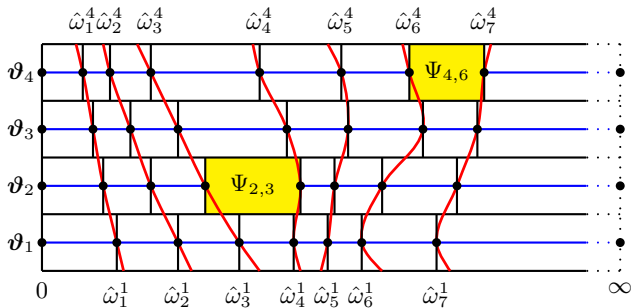$$\Psi_{\alpha,\nu} \xrightarrow{\mathcal{S}_{\alpha,\nu}} \mathcal{X} = [0,1]^{\rho+1}, \tag{11}$$

Fig. 2. Adaptive subdivision of parameter space Θ (vertical axis) for $\rho = 1$ and frequency (horizontal axis). See text for details.

and a local search for the global minimum of the passivity metric $\xi(\boldsymbol{x}) = \eta(\mathcal{S}^{-1}(\boldsymbol{x}))$ with $\boldsymbol{x} \in \mathcal{X}$ is performed.

The main tool is a $(\rho+1)$-dimensional M-tree [7], which is refined through scales h with resolution M^{-h-1} along each direction $\ell = 1, \ldots, \rho + 1$. Refinement follows the simple rule of exploring the *most promising leaf*. At each scale h of the tree the target function ξ is evaluated along one direction ℓ at M children points x_i^ℓ, and the one with the smallest value of ξ is selected for a further refinement along the next direction $\ell + 1$. This operation is repeated until all directions of expansion have been explored. When an *expansion cycle* has been completed ($\ell = \rho + 1$), we determine if the scale of the tree h must be increased or if a *restart* is needed (i.e. a new sequence of expansion is initialized). This decision is triggered by comparing the values attained by the passivity metric to the threshold, through a multivariate generalization of [6]. The algorithm stops when the maximum number of evaluations (*budget*) is reached.

The refinement can be setup in two modes [6]: a *fast mode* providing a binary answer on whether the model is passive or not, in which iterations are stopped as soon as a negative value of the passivity metric is found; an *accurate mode* that continues iterations until an estimate of all negative local minima of ξ are found within a prescribed tolerance.

III. RESULTS

We consider a database of 36 models of integrated devices (capacitors, inductors and transformers), half depending on $\rho = 1$ (cases 1–18) and $\rho = 2$ (cases 19–36) parameters. Passivity of all models was tested using the multivariate Hamiltonian check of [5] and the proposed algorithm. The results of both approaches are documented in Fig. 3. This figure shows that for all cases except one (#32) both approaches were in agreement in detecting passivity violations. For case 32, the Hamiltonian check failed to detect a passivity violation, which was instead found by proposed approach. In some cases (#8 and #20) the local minimum estimate provided by adaptive sampling resulted more accurate.

The real advantages of proposed adaptive sampling scheme become evident when considering runtime. The cumulative CPU time for running all passivity checks on univariate models ($\rho = 1$) was 685 seconds for the Hamiltonian test and 54 seconds for proposed approach. For bivariate models ($\rho = 2$),
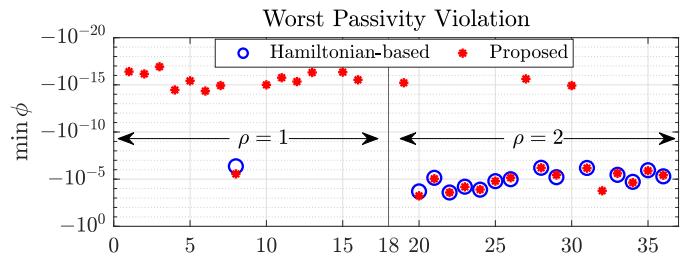

Fig. 3. Worst-case passivity violations identified by the standard Hamiltonian (blue) and proposed (red) passivity checks for all 36 testcases.
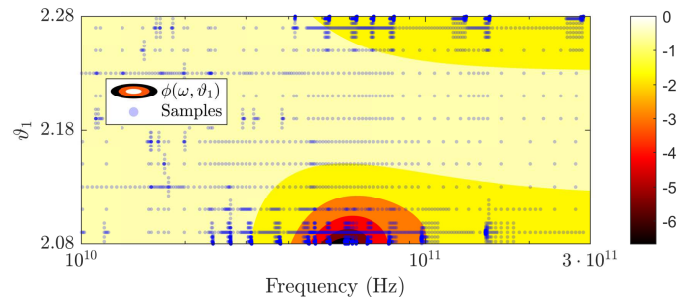

Fig. 4. Adaptive sampling of $\phi(\omega, \boldsymbol{\vartheta})$ for a scattering model (zoomed view with a linear color scale).

total runtime was 6660 and 308 seconds, respectively, resulting in an average speedup of $13\times$ and $22\times$. An illustrative case is depicted in Fig. 4, which represents the passivity metric for a univariate model ($\rho = 1$), highlighting the samples evaluated by proposed algorithm. As expected, these samples crowd near the local minima.

IV. CONCLUSIONS

This paper presented a two-step multiscale adaptive sampling scheme for passivity characterization of parameterized macromodels. For these structures, there are no purely algebraic tools enabling detection of passivity violations. The proposed method was able to correctly identify such violations on 36 models of integrated devices, in much faster runtime than competing approaches based on Hamiltonian matrices.

REFERENCES

[1] S. Grivet-Talocia and B. Gustavsen, *Passive Macromodeling: Theory and Applications*. New York: John Wiley and Sons, 2016.

[2] D. Deschrijver, T. Dhaene, and D. De Zutter, "Robust parametric macromodeling using multivariate orthonormal vector fitting," *IEEE Trans. MTT*, vol. 56, no. 7, pp. 1661–1667, July 2008.

[3] P. Triverio, S. Grivet-Talocia, and M. S. Nakhla, "A parameterized macromodeling strategy with uniform stability test," *IEEE Trans. Adv. Packag.*, vol. 32, no. 1, pp. 205–215, Feb 2009.

[4] S. Grivet-Talocia and R. Trinchero, "Behavioral, parameterized, and broadband modeling of wired interconnects with internal discontinuities," *IEEE Trans. EMC*, vol. 60, no. 1, pp. 77–85, 2018.

[5] A. Zanco et al., "Enforcing passivity of parameterized lti macromodels via hamiltonian-driven multivariate adaptive sampling," *IEEE Trans. ICCAD*, vol. 39, no. 1, pp. 225–238, 2018.

[6] M. De Stefano et al., "A multistage adaptive sampling scheme for passivity characterization of large-scale macromodels," *IEEE Trans. CPMT*, vol. 11, no. 3, pp. 471–484, 2021.

[7] A. Al-Dujaili and S. Suresh, "A Naive multi-scale search algorithm for global optimization problems," *Information Sciences*, vol. 372, pp. 294–312, dec 2016.